Emission Cross Sections and Spectroscopy of Ho^{3+} Laser Channels in KGd(WO$_4$)$_2$ Single Crystal

María Cinta Pujol, Jaume Massons, Magdalena Aguiló, Francesc Díaz, Mauricio Rico, and Carlos Zaldo

Abstract—The spectroscopic properties of Ho^{3+} laser channels in KGd(WO$_4$)$_2$ crystals have been investigated using optical absorption, photoluminescence, and lifetime measurements. The radiative lifetimes of Ho^{3+} have been calculated through a Judd–Ofelt (JO) formalism using 300-K optical absorption results. The JO parameters obtained were $\Omega_2 = 15.35 \times 10^{-20}$ cm^2, $\Omega_4 = 3.79 \times 10^{-20}$ cm^2, $\Omega_6 = 1.69 \times 10^{-20}$ cm^2. The 7–300-K lifetimes obtained in diluted ($8 \cdot 10^{18}$ cm^{-3}) KGW : 0.1% Ho samples are: $\tau(^5F_3) \approx 0.9$ μs, $\tau(^5S_2) = 19$–3.6 μs, and $\tau(^5F_5) \approx 1.1$ μs. For Ho concentrations below 1.5×10^{20} cm^{-3}, multiphonon emission is the main source of non radiative losses, and the temperature independent multiphonon probability in KGW is found to follow the energy gap law $\tau_{ph}^{-1}(0) = \beta \exp(-\alpha \Delta E)$, where $\beta = 1.4 \times 10^{-7}$ s^{-1}, and $\alpha = 1.4 \times 10^3$ cm. Above this holmium concentration, energy transfer between Ho impurities also contributes to the losses. The spectral distributions of the Ho^{3+} emission cross section σ_{EM} for several laser channels are calculated in σ- and π-polarized configurations. The peak σ_{EM} values achieved for transitions to the $^5I_8$ level are $\approx 2 \times 10^{-20}$ cm^2 in the σ-polarized configuration, and three main lasing peaks at 2.02, 2.05, and 2.07 μm are envisaged inside the $^5I_7 \rightarrow {}^5I_8$ channel.

Index Terms—Crystals, holmium, rare-earth compounds, solid lasers, spectroscopy.

I. INTRODUCTION

THE PRESENT development trend of rare-earth solid-state lasers requires media with low excitation thresholds and high impurity admittance, suitable to be excited by the emission of diode lasers. Ho^{3+} has 13 laser channels ranging from $\lambda = 0.55$ to 3.9 μm and it is prone to multi-wavelength emission by cascade de-excitation [1]. The $^5I_7 \rightarrow {}^5I_8$ emission near $\lambda = 2$ μm is of particular interest because of its use in eye-safe systems, medical applications involving coagulative cutting, and welding. The $^5F_4 + {}^5S_2 \rightarrow {}^5I_8$ holmium laser emission near $\lambda = 0.5$ μm is also of interest due to the present requirement for short-wavelength-emitting solid-state lasers. Moreover, green and blue up-conversion holmium emissions have been observed in several hosts upon excitation in red or infrared regions suitable for diode pumping [2]–[4]. This offers new excitation paths for lasing.

Potassium gadolinium tungstate KGd(WO$_4$)$_2$ (KGW) has achieved outstanding relevance as a frequency self conversion laser host by using the stimulated Raman scattering effect because of its very high cubic nonlinearity, $\chi^{(3)} \approx 10^{-13}$ esu [5], [6]. KGd(WO$_4$)$_2$ belongs to the monoclinic system with C2/c symmetry space group, having four unit formula per unit cell. Trivalent rare earth ions substitute for Gd^{3+} at an eight-coordinated site with C$_2$ site symmetry, in which the C$_2$-axis is parallel to the crystallographic [010] axis. The high rare-earth admittance of KGW would allow codoping with several impurities, helping to reduce the laser threshold of Ho^{3+} by sensitizing with several ion combinations: Cr^{3+}, Fe^{3+}, Tm^{3+}, Er^{3+}, Dy^{3+}, Er^{3+}/Tm^{3+}, or Er^{3+}/Tm^{3+}/Yb^{3+} [7].

The Ho^{3+} laser channels so far demonstrated at 300 K in KGW are only $^5I_7 \rightarrow {}^5I_8$ $\lambda = 2.072$ μm [8] and $^5I_6 \rightarrow {}^5I_7$ $\lambda = 2.934$ μm [9]. Therefore, more work is required to realize lasing in other channels and to optimize the system performance in these two.

Despite the interest in KGW : Ho as a laser medium, the spectroscopic knowledge and lasing demonstrations reported so far are scarce, and most of the previous information is limited to temperatures at or above 77 K. This makes difficult a detailed understanding of Ho^{3+} optical properties, especially because of the rather low energy splitting (≤ 320 cm^{-1}) of the fundamental $^5I_8$ level, the final level for 0.55- and 2-μm laser transitions. This low splitting allows an efficient electronic population of $^5I_8$ Stark sublevels different to the fundamental one, and therefore it influences the laser dynamics to a given temperature. In a previous study of optical absorption and photoluminescence (PL) measurements at 10 K, we have provided a detailed list of the Ho^{3+} energy levels and their assignments have been confirmed by crystal field calculations [10]. The aim of this paper is to provide a survey of the Ho^{3+} PL in KGW, serving as a reference for the analysis of lasing properties and the design of the associated optical elements. Experimental studies as a function of the holmium concentration and temperature, as well as the JO formalism, have been used to estimate radiative and non-radiative probabilities, quantum efficiencies and emission cross sections for the transitions responsible for laser channels.

II. EXPERIMENTAL TECHNIQUES

Inclusion–free KGd$_{1-x}$Ho$_x$(WO$_4$)$_2$ single crystals were obtained by a top-seeded solution growth slow-cooling technique using K$_2$W$_2$O$_7$ as the solvent. The growth procedure is described with more details elsewhere [11]. Crystals of typical size 10–15 $\times$ 8–11 $\times$ 4–4.5 (**c** $\times$ **a*** $\times$ **b**) mm^3

Fig. 1.   Unpolarized 300-K optical absorption of KGW : 1%Ho. Inset: potential laser channels of Ho^{3+}.

were pulled using b-oriented seeds from 88.5 $K_2W_2O_7$–11.5 $KGd_{1-x}Ho_x(WO_4)_2$ solutions with four compositions: x = 0.001 (0.1%), 0.01 (1%), 0.03 (3%), and 0.049 (5%).

The level of Gd^{3+} substitution by Ho^{3+} was analyzed by electron probe microanalysis (EPMA) using a CAMECA Camebax SX 50 system. The Ho concentrations obtained in the crystal were 0.59×10^{20} cm^{-3} (1%Ho), 1.65×10^{20} cm^{-3} (3%Ho), and 3.06×10^{20} cm^{-3} (5%Ho). These results yield a distribution coefficient of $K_{Ho} = 0.85$–1. The holmium concentration in the 0.1% Ho-doped KGW sample was estimated from a comparison of the optical absorption intensity to be $0.08\pm0.2 \times 10^{20}$ cm^{-3}.

The unit cell parameters of the $KGd_{0.951}Ho_{0.049}(WO_4)_2$ crystal have been determined by powder X-ray diffraction. In comparison to undoped KGW, the unit cell volume of 5% Ho-doped KGW is decreased less than 0.05%. This result is foreseeable, since the ionic radii of Ho^{3+} and Gd^{3+} are 1.015 and 1.053 Å, respectively. Due to its low magnitude, the Ho-induced lattice contraction has been ignored in the calculation of the Ho concentrations above.

Optical absorption was measured at room temperature in a Varian 5E spectrophotometer. Continuous-wave (CW) PL was excited using ultraviolet (UV) and visible multiline emissions of a Coherent 5-W Ar^+ laser, model Innova 300. The UV excitation regime partially resembles that achieved under pumping by a high-current-operated Xe-lamp. The excitation light intensity was in the 10–200-mW range. The emission was analyzed with a Spex 340E spectrometer ($f = 34$ cm) and detected with a cooled R928 Hamamatsu photomultiplier ($\lambda = 185$–900 nm), a Ge photodiode [model ADC-403 IR ($\lambda = 1.0$–1.7 μm)], or an InSb photovoltaic detector [model Hamamatsu P5968-060 ($\lambda = 1.1$–5.5 μm)]. The latter two were cooled to 77 K. The detector signals were recorded by using a lock-in amplifier. A nitrogen-excited pulsed dye laser was used for CW-PL measurements with resonant excitation and for lifetime measurements. In the lifetime measurements, the emissions were monitored

by using the same spectrometer described above and detected with a GaInAs photomultiplier ($\lambda = 185$–1060 nm, fall time 2 ns) connected to a Tektronix TDS520 digital oscilloscope. The sample temperature was varied in the 7–300 K temperature range by using flowing liquid-He or close-cycled cryostats and the required temperature controllers.

III. EXPERIMENTAL RESULTS

A. Optical Absorption

Following the selection rules imposed by group theory for the local C_2 symmetry of Ho^{3+} in KGW and taking into account that the fundamental level belongs to an A irreducible representation [10], electronic transitions yield polarized spectra, both in absorption and PL. Transitions between levels with same irreducible representation will be observed with light polarization parallel to the C_2-axis (π-spectra), while transitions between levels with different irreducible representation are polarized perpendicular to it (σ-spectra).

This difference with light polarization has, indeed, been observed in the room-temperature optical absorption spectra of KGW : Ho. Fig. 1 shows an average between optical absorption σ- and π-spectra. The inset of Fig. 1 sketches for reference the energy positions of Ho^{3+} levels inferred from 7-K measurements [10] and the laser channels of Ho^{3+}.

The experimental oscillator strengths $f_{\exp}$ are calculated as

$$f_{\exp} = \frac{4\varepsilon_0 mc^2}{Ne^2\overline{\lambda}^2}\Gamma_{JJ'} \tag{1}$$

where

c vacuum speed of the light;
ε_0 dielectric constant;
m, e electron mass and charge, respectively;
$\overline{\lambda}$ average wavelength of the $J \to J'$ transition;
N holmium concentration;

TABLE I
ROOM-TEMPERATURE EXPERIMENTAL OSCILLATOR STRENGTHS f_{exp} DETERMINED FROM ABSORPTION AND CALCULATED f_{cal}
USING THE Ω_k PARAMETERS OBTAINED FROM THE JO ANALYSIS (RMS $= 0.43 \times 10^{-6}$)

Transition $^5I_8 \rightarrow {}^{2S+1}L_J$	λ (nm)	Oscillator strength (x 10^6)				Residuals
		$f_{\text{exp}}, \pi-$	$f_{\text{exp}}, \sigma-$	$\overline{f}_{\text{exp}}$	f_{cal}	Δf_i (x 10^6)
$^5I_7$	1975	1.92 (ED) 0.61 (MD)	2.26 (ED) 0.63 (MD)	2.15 (ED) 0.62 (MD)	2.24 (ED)	0.09
$^5F_5$	648,5	4.69	5,23	5.05	5.28	0.23
$^5S_2 + {}^5F_4$	542	6.30	7.30	6.97	6.20	0.77
$^5F_3$	488	1.57	2.07	1.90	1.65	0.26
$^5F_2 + {}^3K_8$	472,25	2.20	3,15	2.84	3.02	0.18
$^5G_6 + {}^5F_1$	455	74.80	84.54	81.30	81.29	0.01
$^5G_5$	419,5	6.87	6,70	6.76	6.80	0.04

$\Omega_2 = 15.35 \times 10^{-20}$ cm^2	$\Omega_4 = 3.79 \times 10^{-20}$ cm^2	$\Omega_6 = 1.69 \times 10^{-20}$ cm^2

$\Gamma_{JJ'} = \int \alpha(\lambda) \partial \lambda$—room-temperature integrated absorption;

Table I summarizes the measured oscillator strengths for the $^{2S+1}L_J$ multiplets observed in the σ- and π-spectra.

B. JO Calculations

JO theory [12], [13] is often used to determine the radiative rates of the manifold $^{2S+1}L_J$ levels. The oscillator strength for an electric dipole (ED) transition between $4f^n[L, S]J$ and $4f^n[L', S']J'$ states is

$$f_{ED} = \chi \frac{8\pi^2 mc}{3h\overline{\lambda}(2J+1)} S_{JJ'} \tag{2}$$

where $\chi = (n^2 + 2)^2/9n$ (n is the refractive index), h is Planck's constant, and the line strengths are $S_{JJ'} = \sum_{k=2,4,6} \Omega_k |\langle 4f^n[L, S]J\|U^k\|4f^n[L', S']J'\rangle|^2$. Ω_k are the adjustable JO parameters and the reduced matrix elements corresponding to the $J \rightarrow J'$ transition of Ho^{3+}, $\langle\|U^k\|\rangle$, have been tabulated previously [14], [15]. The Ho^{3+} $^5I_8 \leftrightarrow {}^5I_7$ transition also has some magnetic dipole (MD) character. In that case, the MD oscillator strength is given by

$$f_{MD} = \frac{nh}{6mc\overline{\lambda}(2J+1)} \times |\langle 4f^n[L, S]J\|L+2S\|4f^n[L', S']J'\rangle|^2. \tag{3}$$

The matrix elements of the $|L + 2S|$ MD operator were calculated [16], [17], and the total oscillator strength is given by $f_T = f_{ED} + f_{MD}$.

Since the JO theory does not consider the crystal field of the lattice, its application to anisotropic solids requires an average of the experimental optical properties. For this reason and following previous works [18]–[20], we have measured separately the absorption of each polarization configuration and the average $\overline{f}_{\text{exp}}$ set has been calculated as $\overline{f}_{\text{exp}} = (f_{\text{exp}\,\pi} + 2f_{\text{exp}\,\sigma})/3$. In this calculation, we have used the proper refractive indices of KGW at the corresponding $\overline{\lambda}$ of the multiplet [21]. The Ω_k set has been obtained for minimizing the $\sum_{J'}(f_{\text{exp}} - f_{ED})^2$ differences. Table I shows the Ω_k values obtained for

Ho^{3+} in KGW. The quality of the fit is described by the root-mean-square (RMS) deviation, RMS $= [\sum_{i=1}^q (\Delta f_i)^2/(q - 3)]^{1/2}$, where Δf_i are the residuals between the experimental $(\overline{f}_{\text{exp}})$ and calculated (f_{cal}) oscillator strengths, and q is the number of transitions. In spite of a relatively low number of transitions taken into account for the calculations, the RMS deviation in the case of KGd(WO$_4$)$_2$: Ho^{3+} is equal to 4.3×10^{-7}, being similar to the values obtained for other hosts [19], [20].

The Ω_k parameters were further used to calculate the radiative rates ($A_{JJ'}$) of the luminescent transitions according to the formula

$$A_{EDJJ'} = \chi \left[\frac{16\pi^3 e^2}{3h\varepsilon_0\overline{\lambda}^3}\right] \frac{n^2}{(2J+1)}$$
$$\times \sum_{k=2,4,6} \Omega_k |\langle 4f^n[L, S]J\|U^k\|4f^n[L', S']J'\rangle|^2 \tag{4}$$

$$A_{MDJJ'} = \frac{2\pi n^2 e^2}{\varepsilon_0 mc\overline{\lambda}^2} \times f_{MD} \tag{5}$$

[f_{MD} is given by (2)] for ED and MD transitions, respectively.

The $A_{EDJJ'}$ values of the radiative transition rates calculated for Ho^{3+} transitions related to laser channels in the KGW crystal are summarized in Table II. From the whole $A_{EDJJ'}$ set (not given for the sake of brevity), it is possible to obtain the branching ratios $\beta_{JJ'} = A_{JJ'}/\sum_{J'} A_{JJ'}$ and the radiative lifetimes $\tau_r = 1/\sum_{J'} A_{JJ'}$, also given in Table II.

C. PL

Fig. 2 shows an overview of the 7-K Ho^{3+} CW-PL excited by the UV or visible multiline emissions of the Ar$^+$ laser. In the first case, $^3H_5$ and $^3F_4 + {}^3K_6$ Ho^{3+} multiplets are simultaneously excited through 27 548 cm^{-1} ($\lambda = 363$ nm) and 29 895–29 976 cm^{-1} ($\lambda = 334.5$–333.6 nm) laser lines, while in the second, the excitation takes place at the $^5F_2$ multiplet via the 21 008 cm^{-1} (476 nm) laser emission. The PL emissions observed arise from the de-excitation cascade to levels of lower energy. Under these conditions, the spectral assignments are not straightforward due to the great level number of the Ho^{3+} electronic configuration and the possible overlap of emissions

TABLE II

RADIATIVE TRANSITION RATES, $A_{ED,JJ'}$, AND BRANCHING RATIOS, $\beta_{JJ'}$, OF Ho^{3+} EXPECTED LASER CHANNELS IN KGW. RADIATIVE LIFETIMES, τ_{rad}, AND ROOM-TEMPERATURE MEASURED LIFETIMES, τ_{exp}, FOR Ho^{3+} IN 0.1% Ho-DOPED KGW

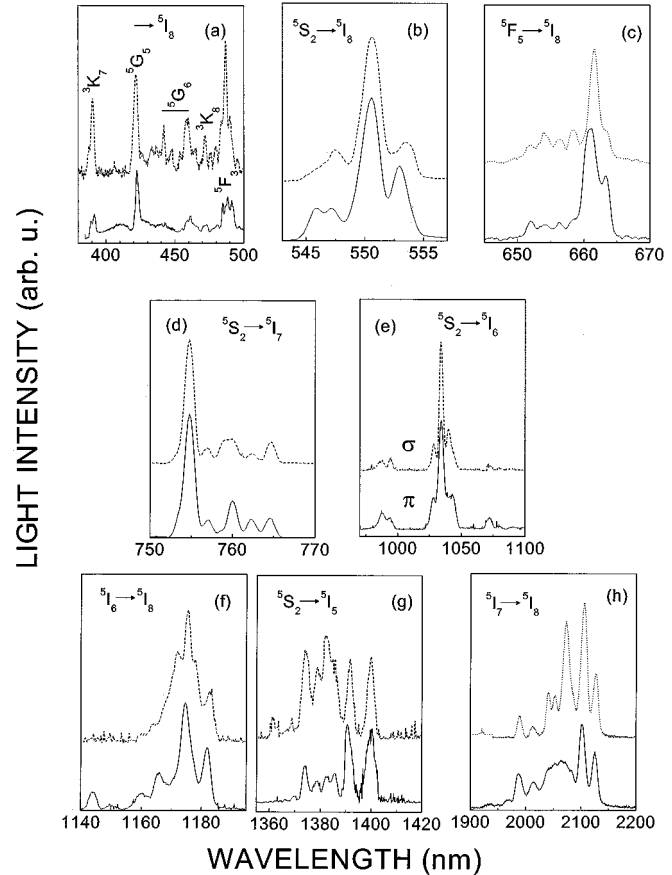|	λ (nm)	$A_{ED,JJ}$ (s^{-1})	$\beta_{JJ'}$ (%)	τ_{rad} (μs)	τ_{exp} (μs)
$^3K_7$				363	
$^5G_4$				16	
$^5G_5$				15	
$^5F_1$				159	
$^5G_6$				6	
$^3K_8$				330	
$^5F_2$				130	
$^5F_3$				89	0.9
$^5F_4$				83	
$^5S_2 \rightarrow {}^5F_5$	3419	1.3	0.02	181	3.6
$^5I_5$	1401	83.8	1.52		
$^5I_6$	1031	369.1	6.67		
$^5I_7$	758	1957.4	35.39		
$^5I_8$	549	3028.8	54.77		
$^5F_5 \rightarrow {}^5I_5$	2374	19	0.28	146	1.1
$^5I_6$	1477	241.9	3.52		
$^5I_7$	974	1331.7	19.39		
$^5I_4$				4692	
$^5I_5 \rightarrow {}^5I_6$	3908	19.5	4.38	2252	
$^5I_7$	1651	192.4	43.34		
$^5I_6 \rightarrow {}^5I_7$	2859	48.3	10.58	2190	
$^5I_8$	1173	408.3	89.42		
$^5I_7 \rightarrow {}^5I_8$	1988	170.6	100.00	5863	

Fig. 2. Overview of Ho^{3+} PL emissions observed in KGW at 7 K and their assignation to electronic transitions. Continuous lines: π-polarized emissions. Dashed lines: σ-polarized emissions. Excitation was performed with the UV and visible multiline emission of an Ar laser.

corresponding to different transitions. In order to eliminate ambiguities in the assignment of the PL bands to electronic transitions, further PL measurements were perfomred with resonant excitation to energy levels below $^5F_2$. For this purpose, a tunable dye laser was used. The correspondence between the observed emission bands and the electronic transitions is given in Fig. 2.

These assignments deserve some comments.

1) The very narrow energy gap between $^5F_4$ and $^5S_2$ levels makes difficult to distinguish their contributions to the green emission at about $\lambda = 545$–555 nm. At 7 K by resonant excitation into the $^5S_2$ level the shape of the emission is very similar to that shown in Fig. 2, therefore most of the emission likely arises from this multiplet. However, it is well known that, at higher temperatures, thermalization of the $^5S_2$ population occurs and $^5F_4 \rightarrow {}^5I_8$ emission, having a higher radiative probability than that for $^5S_2 \rightarrow {}^5I_8$, is observed [22].

2) The emission located in the red, $\lambda = 650$–665 nm, could correspond to the overlapping of $^5F_5 \rightarrow {}^5I_8$ and $^5F_3 \rightarrow {}^5I_7$ transitions. This latter contribution was neglected since the emission shape does not change when the $^5S_2$ multiplet is excited.

3) The emission in the near-infrared region $\lambda = 750$–770 nm arises from the $^5F_4 + {}^5S_2 \rightarrow {}^5I_7$ transition with thermal considerations similar to those mentioned before. Contribution from the $^5I_4 \rightarrow {}^5I_8$ transition were neglected in view of the lacking emission excitation at the $^5F_5$ multiplet.

D. Up-Conversion

PL from the $^5S_2$ level has been also obtained by up-conversion exciting the $^5I_4$ multiplet. The emission spectral distribution obtained at 7 K (not shown for the sake of brevity) is similar to that shown in Fig. 2(b). Fig. 3 shows a comparison between the excitation spectra of this IR-excited $^5S_2$ PL and the ground state absorption (GSA) of the $^5I_4$ multiplet. It is worth remarking that the excitation peaks matching the $^5I_4$ GSA spectrum have very weak intensities.

E. Lifetime Measurements

Lifetimes of several multiplets were obtained by resonant excitation on the high-energy side of $^5F_3$ ($\lambda_{exc} = 484.5$ nm), $^5F_4 + {}^5S_2$ ($\lambda_{exc} = 540.5$ nm) and $^5F_5$ ($\lambda_{exc} = 642$ nm) multiplets. At the lowest Ho concentration available, namely 0.1%, the intensity decays obtained were single exponential, independently of the sample temperature (7–300 K). This single exponential law was also observed for 1% and 3% Ho-doped samples; however, some departure from the exponential law is observed for 5% Ho doping. Fig. 4(a) shows this behavior for the intensity decays of the $^5S_2$ multiplet in 0.1%, 1%, 3%, and 5% Ho-doped samples. The decays of 0.1%–3% Ho-doped samples overlap, giving a $\tau_{exp}({}^5S_2, 7 K) \approx 19 \mu$s.

The experimental lifetime τ_{exp} is related to the radiative lifetime τ_{rad} of the level and its nonradiative probability τ_{NR}^{-1} by
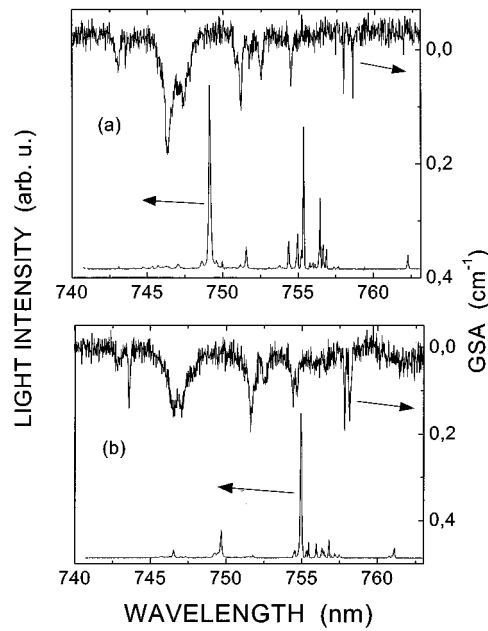
Fig. 3. Comparison between the 7-K up-conversion excitation of the $^5S_2$ PL and the corresponding GSA of the $^5I_4$ multiplet. KGW : 5%Ho.

$\tau_{\exp}^{-1}(T) = \tau_{\text{rad}}^{-1} + \tau_{\text{NR}}^{-1}(T)$. The nonradiative probability is expressed as $\tau_{\text{NR}}^{-1}(T) = \tau_{\text{ph}}^{-1}(T) + \tau_{\text{ET}}^{-1}$, where $\tau_{\text{ph}}^{-1}(T)$ is the multiphonon emission probability and τ_{ET}^{-1} is the energy transfer probability. For a sufficiently large Ho–Ho distance, τ_{ET}^{-1} is negligible and the light intensity decay becomes single exponential; therefore, the results of Fig. 4(a) suggest that at the 0.1% Ho doping level, energy transfer can be ignored.

Lifetime shortening related to electron relaxation by phonon emission has a probability $\tau_{\text{ph}}^{-1}(T) = \tau_{\text{ph}}^{-1}(0) \prod_i (1 + n_i)^{\text{ph}_i}$, where $n_i = [\exp(\overline{h}\omega_i/k_B T) - 1]^{-1}$, k_B is Boltzmann's constant, and ph_i is the number of phonons with energy $\overline{h}\omega_i$ created in the nonradiative transition between levels separated by $\Delta E = \Sigma_i \text{ph}_i \overline{h}\omega_i$.

The expected τ_{rad} values for Ho^{3+} multiplets were provided in Table II. The experimental lifetimes of the $^5F_3$ and $^5F_5$ multiplets have been found to be nearly temperature independent in the 7–300 K range, and the values obtained have been included in Table II. However, a temperature dependent lifetime was obtained for the emission starting in the $^5F_4$ and $^5S_2$ multiplets [see Fig. 4(b)]. For these levels, another source of temperature dependence for the lifetime is the thermal redistribution of the $^5S_2$ electronic population with the $^5F_4$ multiplet lying only $\Delta E = 57$ cm^{-1} above [10]. In that case, the radiative probability becomes $\tau_{\text{rad}}^{-1}(T) = [g_1\tau_{\text{rad1}}^{-1}\exp(-\Delta E/k_B T) + g_2\tau_{\text{rad2}}^{-1}][g_1\exp(-\Delta E/k_B T) + g_2]^{-1}$, g_1 and g_2 being the degeneracies of the $^5F_4$ and $^5S_2$ multiplets, respectively.

Fig. 4(b) shows the fit of the experimental $^5F_4 + ^5S_2$ lifetimes, taking into account the electron population redistribution and phonon emission. The assumption of 3 phonon ($\overline{h}\omega = 901$ cm^{-1}) emission is not able to reproduce the temperature lifetime dependence. Emission of phonons with lower energy is required to roughly reproduce the thermal behavior of this lifetime.

The temperature independent multiphonon probability follows the energy gap law $\tau_{\text{ph}}^{-1}(0) = \beta\exp(-\alpha\,\Delta E)$, where β
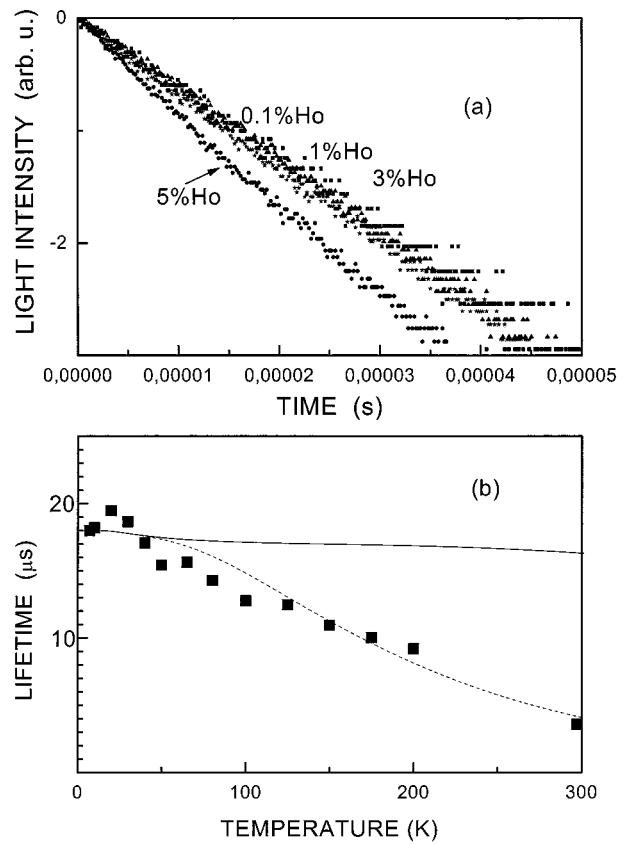

Fig. 4. (a) Low temperature (7 K) PL decay of the $^5S_2$ multiplet as a function of the Ho concentration in KGW. (b) Temperature dependence of the PL lifetime of the $^5S_2$ multiplet for 0.1% Ho-doped KGW. $\lambda_{\text{EMI}} = 540.5$ nm , $\lambda_{\text{EXC}} = 550$ nm.
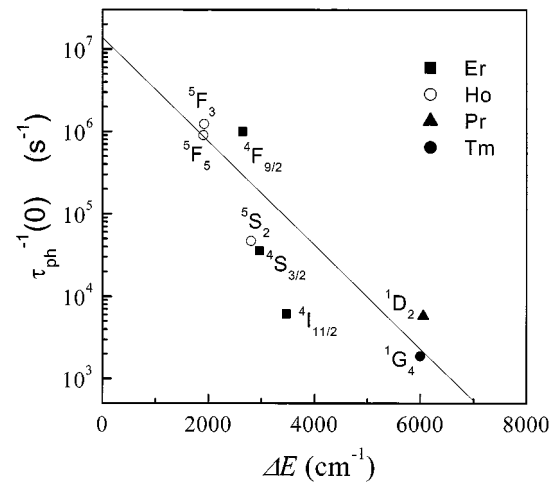

Fig. 5. Energy gap law of the temperature-independent nonradiative phonon-emission probability for the KGW laser host.

and α are characteristic of the host. A previous attempt to characterize α and β parameters in KGW was based only on three lifetimes of Er^{3+} [21]. Fig. 5 shows a recalculation of these parameters on the base of Pr^{3+} [23], Ho^{3+} (this work), Er^{3+} [21], and Tm^{3+} [24] lifetimes, which cover a broad range in ΔE. The best fit of the results of Fig. 5 yields $\beta = 1.4 \times 10^7$ s^{-1} and $\alpha = 1.4 \times 10^{-3}$ cm.
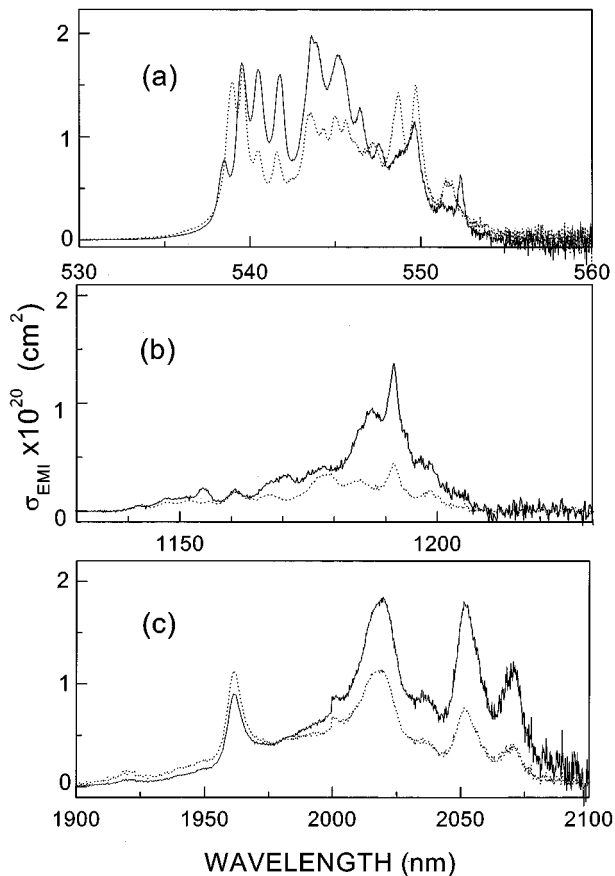
Fig. 6. Emission cross sections σ_{EMI} of Ho^{3+} in KGW. (a) $^5F_4 + {}^5S_2 \to {}^5I_8$ laser channel. (b) $^5I_6 \to {}^5I_8$ laser channel. (c) $^5I_7 \to {}^5I_8$ laser channel. Continuous and dashed lines: σ- and π-polarized configurations.

IV. DISCUSSION

The laser efficiency of a rare earth-doped solid-state material is related to the intrinsic radiative properties of the rare earth ion and to the losses due to nonradiative processes. Fig. 2 has identified the relevant electronic transitions contributing to a particular emission band of Ho^{3+} in KGW. Once the initial and final Ho^{3+} levels of the transition are known and ignoring the nonradiative processes, it is possible to estimate the emission cross sections $\sigma_{EM}(\lambda)$ for the three Ho^{3+} laser channels terminating on the ground $^5I_8$ multiplet. To this purpose, we use the experimental GSA cross section $\sigma_{GSA}(\lambda) = \alpha(\lambda)/N$ and the reciprocity principle [25]

$$\sigma_{EMI} = \sigma_{GSA} \frac{Z_l}{Z_u} e^{(E_{zl} - h\nu)/k_B T} \qquad (6)$$

where Z_u and Z_l are the partition functions of the upper and lower multiplets, respectively, and E_{zl} is the energy difference between the lowest Stark levels of these two multiplets.

Fig. 6 shows the spectral dependence of the room temperature σ_{EMI} for $^5F_4 + {}^5S_2 \to {}^5I_8$ ($\lambda \approx 550$ nm), $^5I_6 \to {}^5I_8$ ($\lambda \approx 1.2$ μm), and $^5I_7 \to {}^5I_8$ ($\lambda \approx 2$ μm) laser channels.

As a first approximation, light amplification could be expected when the emitted light counterbalances the absorption losses. If P is the population fraction of the excited state, this condition can be described as $P\sigma_{EMI} - (1 - P)\sigma_{GSA} > 0$.
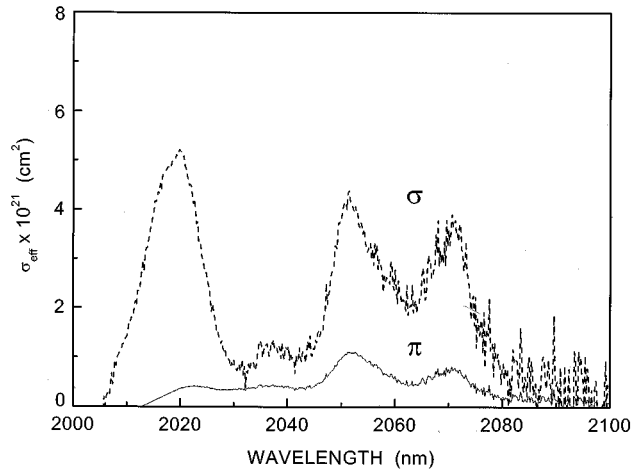

Fig. 7. Effective emission cross section, $\sigma_{EFF} = P\sigma_{EMI} - (1 - P)\sigma_{GSA}$, for the $^5I_7 \to {}^5I_8$ laser channel of Ho^{3+} in KGW for σ- and π-polarized configurations. P $= 0.4$.

Fig. 7 shows this condition for different polarization configurations in the 2-μm laser channel. Three emission maxima can be expected at about 2020, 2051, and 2071 nm and, in all cases, the selection of σ-polarized emission is favored. It is worth remarking that the maximum at 2071 nm agrees very well with the $\lambda = 2072$-nm laser emission actually found in KGW : Ho [8]. This builds confidence in the simulation of Fig. 7 and should encourage further search of the other possible lasing peaks in this channel.

The peak σ_{EMI} obtained for Ho^{3+} in KGW is $\approx 2 \times 10^{-20}$ cm^2 (see Fig. 6). This value compares well to those reported in other laser hosts, namely, $\sigma_{EMI} \approx 1.84 \times 10^{-20}$ cm^2 for LiYF$_4$ to $\sigma_{EMI} \approx 0.28 \times 10^{-20}$ cm^2 for KCaF$_3$ [26]. Therefore, efficient laser operation appears possible. However, the nonradiative processes also limit the laser efficiency. In this respect, the KGW lattice has a large energy value of the highest Raman phonon ($\overline{h}\omega \approx 901$ cm^{-1}) and a rich phonon spectrum. In fact, it is clear from Fig. 4 that multiphonon emission is rather relevant, decreasing the radiative emission efficiency. The $^5F_4 + {}^5S_2$ luminescence quantum yield at room temperature, $\eta = \tau_{\exp}/\tau_{\rm rad} \approx 0.02$, is rather low; therefore, codoping with sensitizing ions should be relevant for efficient laser action. In this respect, the KGW crystal is a good host due to its high rare-earth acceptance level. Generally, 5% rare-earth doping has been achieved without losing optical quality [11]. According to the results of Fig. 4(a), the holmium concentration can be increased up to about 3% without significant enhancement of the Ho–Ho energy migration losses and, therefore, the crystals can be co-doped with a further 2% of other sensitizing ions, Tm^{3+} being the most commonly used.

Another source of losses which may particularly influence the $^5I_7 \to {}^5I_8$ ($\lambda \approx 2$ μm) emission yield during optical pumping with diodes is up-conversion. Fig. 3 has evidenced this process in our KGW : Ho samples. The up-conversion excitation may arise from different processes, such as ESA, energy transfer from Ho neighbors (ETU), or photon avalanche [27]. In view of the poor matching between GSA and the up-conversion excitation, the ETU process seems to be less relevant than is excited-state absorption by intermediate levels.

V. CONCLUSION

The relevant electronic transitions contributing to Ho^{3+} PL in KGW single crystals have been identified in the 7–300 K temperature range. The radiative lifetimes of the $^5F_3$, $^5S_2$, and $^5F_5$ levels of Ho^{3+} are about two orders of magnitude larger than those measured. This difference has been associated mainly with strong multiphonon de-excitation due to the relatively small energy gaps between holmium multiplets and the large energy of KGW phonons. Energy transfer between Ho impurities becomes important for impurity concentrations above 3×10^{20} cm^3. The peak emission cross sections for the laser channels terminating on the ground $^5I_8$ multiplet are 2×10^{-20} cm^2. This suggests three main laser-tuning regions ($\lambda \approx 2.02, 2.05, 2.07 \ \mu$m) inside the $^5I_7 \rightarrow {}^5I_8$ laser channel.

REFERENCES

[1] A. A. Kaminskii, *Crystalline Lasers: Physical Processes and Operating Schemes*. Boca Raton, FL: CRC, 1996, pp. 41–44.

[2] X. Zhang, X. Liu, J. P. Jouart, and G. Mary, "Upconversion fluorescence of Ho^{3+} ions in a BaF$_2$ crystal," *Chem. Phys. Lett.*, vol. 287, pp. 659–662, 1998.

[3] D. N. Patel, B. R. Reddy, and S. K. Nashstevenson, "Spectroscopy and two-photon upconversion studies of Ho^{3+}-doped Lu$_3$Al$_5$O$_{12}$," *Opt. Mat.*, vol. 10, pp. 225–234, 1998.

[4] M. Malinowski, R. Piramidowicz, Z. Frukacz, G. Chadeyron, R. Mahiou, and M. F. Joubert, "Spectroscopy and upconversion processes in YAlO$_3$: Ho^{3+} crystals," *Opt. Mat.*, vol. 12, pp. 409–423, 1999.

[5] I. V. Mochalov, "Nonlinear optics of the potassium gadolinium tungstate laser crystal Nd^{3+} : KGd(WO$_4$)$_2$," *J. Opt. Technol.*, vol. 62, pp. 746–756, 1995.

[6] J. Findeisen, H. J. Eichler, and A. A. Kaminskii, "Efficient picosecond PbWO$_4$ and 2-wavelength KGd(WO$_4$)$_2$ Raman lasers in the IR and visible," *IEEE J. Quantum Electron.*, vol. 35, pp. 173–178, 1999.

[7] G. Rustad and K. Stenersen, "Modeling of laser pumped *Tm* and *Ho* lasers accounting for upconversion and ground state depletion," *IEEE J. Quantum Electron.*, vol. 32, pp. 1645–1656, 1996.

[8] A. A. Kaminskii, A. A. Pavlyuk, P. V. Klevtsov, I. F. Balashov, V. A. Berenberg, S. E. Sarkisov, V. A. Fedorov, M. V. Petrov, and V. V. Lyubchenko, "Stimulated radiation of monoclinic crystals of KGd(WO$_4$)$_2$ with Ln^{3+} ions," *Izv. Akad. Nauk. SSSR Neorgan. Mat.*, vol. 13, pp. 582–583, 1977.

[9] A. A. Kaminskii, A. A. Pavlyuk, T. I. Butaeva, K. N. Fedorov, I. F. Balashov, V. A. Berenberg, and V. V. Lyubchenko, "Stimulated emission by subsidiary transitions of Ho^{3+} and Er^{3+} in KGd(WO$_4$)$_2$," *Izv. Akad. Nauk. SSSR Neorgan. Mat.*, vol. 13, pp. 1541–1542, 1977.

[10] M. C. Pujol, C. Cascales, M. Rico, J. Massons, F. Díaz, P. Porcher, and C. Zaldo, "Measurement and crystal field analysis of energy levels of Ho^{3+} and Er^{3+} in KGd(WO$_4$)$_2$ single crystal," *J. Alloys Comp.*, vol. 323–324, pp. 321–325, 2001.

[11] M. C. Pujol, R. Solé, Jna. Gavaldá, J. Massons, M. Aguiló, F. Díaz, V. Nikolov, and C. Zaldo, "Growth and ultraviolet optical properties of KGd$_{1-x}$RE$_x$(WO$_4$)$_2$ single crystals," *J. Mater. Res.*, vol. 14, pp. 3739–3745, 1999.

[12] B. R. Judd, "Optical absorption intensities of rare-earth ions," *Phys. Rev.*, vol. 127, pp. 750–761, 1962.

[13] G. S. Ofelt, "Intensities of crystal spectra of rare-earth ions," *J. Chem. Phys.*, vol. 37, pp. 511–520, 1962.

[14] M. J. Weber, B. H. Matsinger, V. T. Donlan, and G. T. Surratt, "Optical transition probabilities for trivalent holmium in LaF$_3$ and YAlO$_3$," *J. Chem. Phys.*, vol. 57, pp. 562–567, 1972.

[15] W. T. Carnall, P. R. Fields, and K. Rajnak, "Electronic energy levels in the trivalent lanthanide aquo ions—Part I: Pr^{3+}, Nd^{3+}, Sm^{3+}, Dy^{3+}, Ho^{3+}, Er^{3+} and Tm^{3+}," *J. Chem. Phys.*, vol. 49, pp. 4424–4442, 1968.

[16] M. J. Weber, "Probabilities for radiative and nonradiative decay of Er^{3+} in LaF$_3$," *Phys. Rev.*, vol. 157, pp. 262–272, 1967.

[17] W. T. Carnall, P. R. Fields, and B. G. Wybourne, "Spectral intensities of the trivalent lanthanides and actinides in Solution—Part I: Pr^{3+}, Nd^{3+}, Er^{3+}, Tm^{3+} and Yb^{3+}," *J. Chem. Phys.*, vol. 42, pp. 3797–3806, 1965.

[18] B. M. Walsh, N. P. Barnes, and B. di Bartolo, "Branching ratios, cross-sections, and radiative lifetimes of rare-earth ions in solids—Application to Tm^{3+} and Ho^{3+} ions," *J. Appl. Phys.*, vol. 83, pp. 2272–2787, 1998.

[19] A. Lorenzo, L. E. Bausá, J. A. Sanz-García, and J. Garcia Solé, "Optical absorption intensities and fluorescence dynamics of Ho^{3+} ions in LiNbO$_3$," *J. Phys.: Condens. Matter.*, vol. 8, pp. 5781–5791, 1996.

[20] G. Dominiak-Dzik, S. Golab, J. Zawadzka, W. Ryba-Romanowski, T. Lukasiewicz, and M. Swirkowicz, "Spectroscopic properties of holmium doped LiTaO$_3$ crystals," *J. Phys.: Cond. Matt.*, vol. 10, pp. 10 291–10 306, 1998.

[21] M. C. Pujol, M. Rico, C. Zaldo, R. Solé, V. Nikolov, X. Solans, M. Aguiló, and F. Díaz, "Crystalline structure and optical spectroscopy of Er^{3+}-doped KGd(WO$_4$)$_2$ single crystals," *Appl. Phys. B*, vol. 68, pp. 187–197, 1999.

[22] B. Moine, A. Brenier, and C. Pedrini, "Fluorescence dynamics of Er^{3+} and Ho^{3+} ions and energy transfer in some fluoride glasses," *IEEE J. Quantum Electron.*, vol. 25, pp. 88–96, Jan. 1989.

[23] C. Zaldo, M. Rico, C. Cascales, M. C. Pujol, J. Massons, M. Aguiló, F. Díaz, and P. Porcher, "Optical spectroscopy of Pr^{3+} in KGd(WO$_4$)$_2$ single crystals," *J. Phys. Cond. Matt.*, vol. 12, pp. 8531–8550, 2000.

[24] M. C. Pujol, "Obtenció i caracterització de cristalls monoclínics de KGd(WO$_4$)$_2$ substituïts amb lantànids," Ph.D. dissertation (in Catalan), Univ. Rovira i Virgili, Tarragona, Spain, 2001.

[25] D. E. McCumber, "Einstein relations connecting broadband emission and absorption spectra," *Phys. Rev.*, vol. 136, pp. A954–A957, 1964.

[26] S. A. Payne, L. L. Chase, L. K. Smith, W. L. Kwag, and W. F. Krupke, "Infrared cross-section measurements for crystals with Er^{3+}, Tm^{3+} and Ho^{3+}," *IEEE J. Quantum Electron.*, vol. 28, pp. 2619–2630, 1992.

[27] G. K. Liu, Y. H. Chen, and J. V. Beitz, "Photon avalanche up-conversion in Ho^{3+} doped fluoride glasses," *J. Lumin.*, vol. 81, pp. 7–12, 1999.

María Cinta Pujol received the Ph.D. degree in chemistry from the University Rovira i Virgili, Tarragona, Spain, in 2001, with a thesis on growth and characterization of monoclinic crystals of KGd(WO$_4$)$_2$ modified with lanthanides.

Jaume Massons was born in Lleida, Spain, in 1959. He received the Ph.D. degree in physics from Barcelona University, Barcelona, Spain, in 1987.

He is currently a Senior Lecturer of Applied Physics at the University of Tarragona, Tarragona, Spain. His research interests include optical spectroscopy of rare-earth ions for laser applications and nonlinear optical processes, such as cooperative luminescence and step-up conversion.

Magdalena Aguiló was born in Sa Pobla, Mallorca, Spain, in 1953. She received the Ph.D. degree in physics from Barcelona University, Barcelona, Spain, in 1983.

Currently, she is Professor of Crystallography at the University Rovira i Virgili, Tarragona, Spain, where she is researching crystallography, crystal growth, X-ray diffraction, X-ray texture analysis, and physical properties in relation with the crystalline structure.

Francesc Díaz was born in Lugo, Spain, in 1953. He received the Ph.D. degree in physics from Barcelona University, Barcelona, Spain, in 1982. Currently, he is Professor of Applied Physics at the University Rovira i Virgili, Tarragona, Spain. His research interest includes spectroscopy (absorption and emission) of rare-earth ions for laser applications and nonlinear optical processes, such as cooperative luminescence and step-up conversion.

Mauricio Rico was born in Logroño, Spain, in 1973. He received the B.Sc. degree in physics from Autonomous University, Madrid, Spain, in 1997. He is currently working toward the Ph.D. degree in physics at the Institute of Materials Science, Madrid, Spain, under a fellowship.

He is the author of 14 works on optical spectroscopy of rare-earth ions in KTP and double-tungstate or molibdate crystalline hosts.

Carlos Zaldo was born in Madrid, Spain, in 1956. He received the Ph.D. degree in physics from Autonomous University, Madrid, Spain, in 1984.

After postdoctoral research on photorefractive materials at ETH-Zürich, Switzerland, in 1986 he joined the Institute of Materials Science, Madrid, Spain, as part of the Spanish Research Council. He presently holds a Scientist Research Chair. He has taught spectroscopy and photonics matters at Autonomous University and Carlos III University, Madrid, Spain. He is the author of more than 100 international publications in the fields of bulk and thin-film preparation of ferro/piezoelectric or optical materials and spectroscopies. His current research activities are focused on films (ZnO, $PbTiO_3$-related, $KNbO_3$, $LiNbO_3$ and $Bi_{12}GeO_{20}$-like) prepared by pulsed laser deposition, their characterization and integration with Si and InP semiconductors; optical spectroscopy and laser properties of rare earth ions in non-linear single crystal hosts—KTP, $NdAl_3(BO_3)_4$, $KGd(WO_4)_2$, $BiGeY_{1-x}RE_xGe_5$ and $Li/NaBi(W/MoO_4)_2$.

Dr. Zaldo is a member of the OSA and E-MRS societies.